Flavobacterium johnsoniae Tyrosine Ammonia Lyase (Fjtal) *In-Silico* Structure Prediction and Molecular Docking to L-Tyrosine, P-Coumaric Acid (pHCA) and Caffeic Acid

Seyyed Amirrez Mousavi Majda*

Department of Biotechnology, College of Science, University of Tehran, Tehran, Iran

ABSTRACT

Responsible for the conversion of L-tyrosine to p-coumaric acid in *Flavobacterium johnsoniae*, FjTAL has drawn the attention of many biochemical engineers who wish to carry out a sustainable biosynthetic scheme for the production of aromatic compounds. In this study, with the aid of various computational tools, the secondary and tertiary structures of FjTAL have been predicted. The results suggest that FjTAL forms a homo-tetramer when active as a cytosolic enzyme and it is mostly consisted of alpha helices. With the aid of molecular docking, one can hypothesize that FjTAL is likely to bind to L-tyrosine, p-coumaric acid, and caffeic acid with a similar molecular mechanism and thus, p-coumaric acid and caffeic acid may exhibit a negative feedback response toward the enzyme and inhibit its activity competitively. Two distinct binding pockets have been discovered, one of which contains highly conserved residues among several species. The residues which form the prosthetic group 3, 5-dihydro-5-methylidene-4H-imidazol-4-one (MIO) also emerge in the evolutionary conserved binding pocket. The other discovered cavity could either be a second binding site for the ligands or simply an artifact of the molecular docking task.

Keywords: Protein structure prediction; Computational biology; Tyrosine Ammonia Lyase (TAL); *Flavobacterium johnsoniae* Tyrosine Ammonia Lyase (FjTAL)

INTRODUCTION

In the recent methods that have been developed for the sustainable production of phenylpropanoids in recombinant *E. coli*, FjTAL has been proposed as one of the potential enzymes to convert L-tyrosine to p-coumaric acid (Figure 1) [1-3].

Although it has been demonstrated that *Flavobacterium johnsoniae* Tyrosine Ammonia Lyase (FjTAL), has satisfactory affinity for L-tyrosine (Km~6.7 μM), little has been reported on the binding affinity of other structurally-related metabolites to FjTAL [4,5]. It has been hypothesized by Sariaslani (2007) [6] and Haslinger and Prather (2020) that p-coumaric acid, the product of elimination reaction catalyzed by FjTAL, might inhibit the activity of the enzyme, exerting a kind of negative feedback response. The goal of this study is to computationally predict the 3D structure of FjTAL, paving the way to help other researchers to reasonably engineer the protein for the future studies. It is worth mentioning that since not even a single experimental data on the structure of the enzyme in Protein Data Bank (PDB) was available, one had to only rely on computational methods in order to determine the structure of the enzyme.
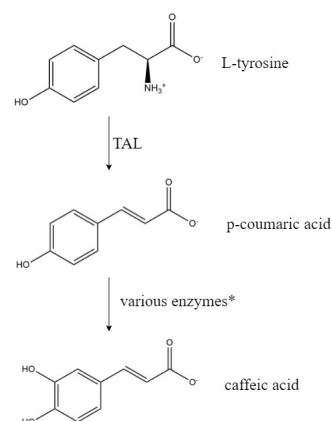

Figure 1: The artificial biosynthetic pathway developed by Rodrigues et al. (2015)2 and Haslinger and Prather (2020)1 and the structure of related metabolites at pH=7.4, TAL: Tyrosine Ammonia Lyase, Ex: FjTAL, RgTAL, SeSam8, RsTAL, HaTAL. *Many different enzymes are utilized for the next step of the artificial pathway including CYP199A2, 4-coumarate 3-hydroxylase, hydroxyphenylacetate 3-hydroxylase.

The *in-silico* experiment design

The general strategy devised in this study is depicted in Figure 2. To predict the 3D structure of FjTAL, the sequence of the enzyme had to be retrieved. The codon-optimized DNA sequence of FjTAL was retrieved from the supplementary file of Haslinger and Prather (2020) [1], and translated it into amino acid alphabet by using the Biostrings package [7]. It was also observed that a record had already existed in NCBI with the exact sequence (SCV44818.1 unnamed protein product).With the FjTAL protein sequence available, four webservers were employed in order to predict tertiary structure of FjTAL. Two of these webservers, SWISS-MODEL [8-12] and Phyre212, implement homology modelling algorithms while the other two, AlphaFold2 [13-15] and RoseTTAFold [16], predict the structures without the aid of template (ab-initio prediction). FjTAL protein sequence was fed into each of these four servers. Then, the quality of these structures was validated using the SAVES of UCLA [17-19] and the ones that did not meet the standards were eliminated. Eventually, the top five pdb files which were found to be superior among all, were stored as pdb files for the next steps. After that, the secondary structures of the predicted models were extracted from the pdb files and secondary structure prediction methods that were only dependent on the input sequence rather than tertiary structure (Figure 2).

Figure 2: The workflow carried out in this study.
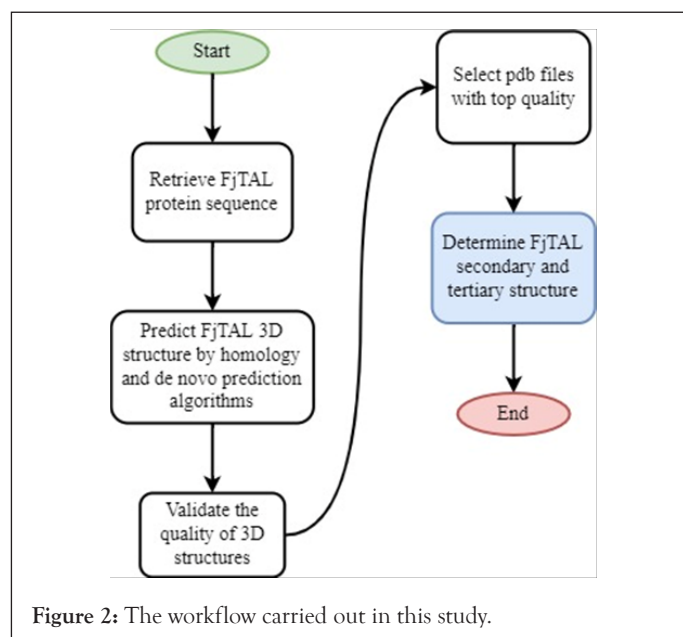
MATERIALS AND METHODS

TIn this study quite a few computational tools were employed to help us fulfill the computational experiment. In brief, the workflow started with employing Biostring package to retrieve the sequence of FjTAL. Then the tertiary structure prediction was done by using Phyre2, SWISS-MODEL as well as ColabFold and Robetta. SAVES of UCLA was helpful in ranking the predicted structures. The molecular docking task (see section 3.3) was executed by CB-Dock and the results were subsequently analyzed by ChimeraX, Mol* and BIOVIA. The complete list of the software and webservers is given in Table 1.

Table 1: The list of computational tools used throughout this survey. Mol* is used to determine the residues that constituted the binding pocket of FjTAL in each of these complexes.

Task	Database/Webserver/Software
DNA to AA translation	Biostrings (R)
Tertiary structure prediction	Homology modelling: Phyre2, SWISS-MODEL
	Ab-initio modelling: ColabFold (a light version of AlphaFold2 with the help of AMBER forcefield), Robetta (webserver hosting a version of RoseTTAFold)
.pdb file quality assessment	SAVES of UCLA
Secondary structure retrieval from .pdb files	Stride
Secondary structure prediction (sequence input only)	JPred4, PROTEUS2
Superimpose structures and calculate RMSD	BIOVIA Discovery Studio
.pdb file viewer	Chimera X, Mol*
Ligands .mol files retrieval	ChemSpider
Add/Remove proton to ligands .mol files (pH=7.4)	Galaxy servers, Open Babel, Pybel
Ligands MM2 minimization	Chem3D
Blind molecular docking	CB-Dock, a blind docking tool based on AutoDock Vina
Miscellaneous	ChemDraw, draw.io, GraphPad Prism

RESULTS AND DISCUSSION

FjTAL structure prediction and quality assesment

As mentioned before, four webservers were employed to predict the structure of FjTAL. Phyre2, SWISS-MODEL, ColabFold and Robetta generate one, two, five and five structures respectively. It is worth noting that ColabFold initially generates five unrelaxed structures and five AMBER-relaxed structures which we used only the latter for the purposes of this study. SWISS-MODEL also predicted that FjTAL is likely to be either a homotetrameric or a homodimeric protein. However, most of the closely-related homologs of FjTAL were proven to be homotetrameric and thus, we have concluded this may also be a valid assumption for FjTAL as well.

All thirteen pdb files were passed to SAVES webserver to assess the quality of the predicted structures. The ideal structures had to pass Verify3D test and achieve a score<>95 in ERRAT program (top five structures were selected) (Table 2).

As shown in Table 2, ab-initio algorithms significantly outperformed Phyre2 and SWISS-MODEL. The superiority of AlphaFold2 and RoseTTAFold over classical methods had also been proposed in other studies such as CAMEO [20-22] as well. The top five structures were selected and stored.

Table 2: The results of quality assessment using SAVES. FjTAL_Final_Phyre2.pdb is the file generated on Phyre2 server. FjTAL_X_SWISS.pdb files are the output of SWISS-MODEL. FjTAL_X_Rob.pdb files are the tertiary structures predicted by Robetta/RoseTTAFold. FjTAL_X_AF2 files are the output of ColabFold/AlphaFold2.

	Errat	Verify
FjTAL_Final_Phyre2	79.5181	PASS
FjTAL_2_SWISS	89.7918	PASS
FjTAL_1_SWISS	89.9897	FAIL
FjTAL_5_Rob	93.7374	PASS
FjTAL_1_Rob	94.5122	PASS
FjTAL_2_Rob	95.3157	PASS
FjTAL_2_AF2	95.6701	PASS
FjTAL_5_AF2	96.0986	PASS
FjTAL_3_Rob	96.5726	PASS
FjTAL_4_AF2	97.9381	PASS
FjTAL_1_AF2	97.9508	PASS
FjTAL_4_Rob	97.9633	PASS
FjTAL_3_AF2	98.5714	PASS

FjTAL secondary and tertiary structure

The top models from previous sections (yellow highlights in Table 2) were passed to Stride22 to extract the secondary structures from pdb files.

We also tried to predict the secondary structures using JPred4 [23] and PROTEUS2 [24] webservers which require the protein sequence as their only input (Table 3).

In Table 3 the prediction results by JPred4, PROTEUS2 and the extraction results by Stride are tabulated. As shown in Table, while, to some extents, the results differ from one model to another, one can state that FjTAL is mostly consisted of alpha helices with very few, short length, beta strands.
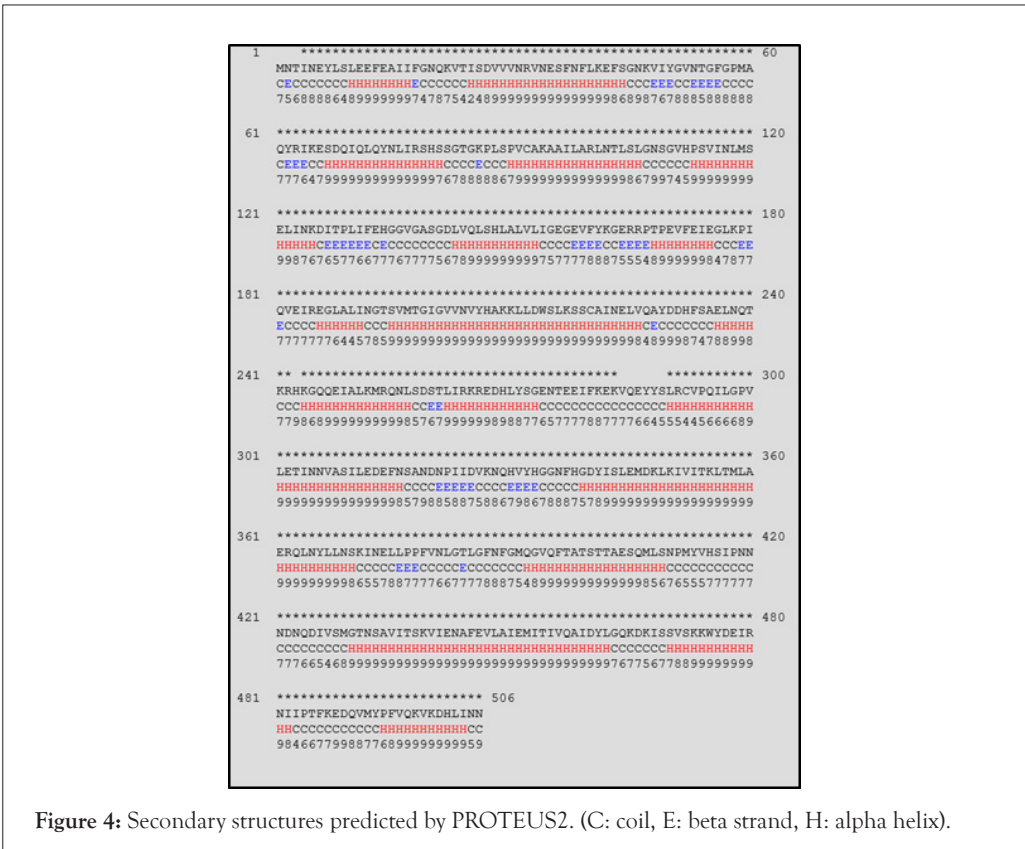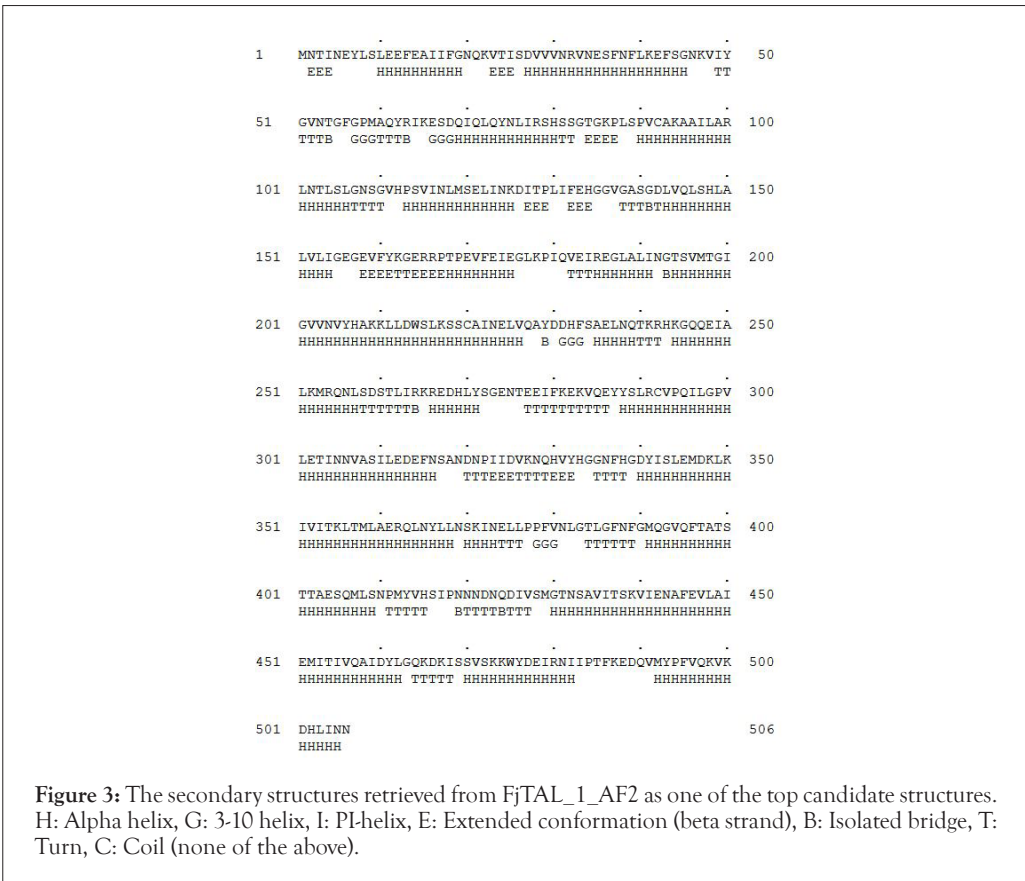
Note that JPred4 and PROTEUS2 do not generate any data on the number of 310 helices that may exist in the structures and also notice that the number of beta strands differ significantly in each record, mainly because FjTAL seems to have very short (length=<4 amino acid) beta strands. This has led to emergence of presumably false positive results in the case of beta strands especially in the prediction-based results (Figures 3 and 4).

The structure of FjTAL_1_AF2 is shown in Figure 5 as an example [25,26]. We also passed the pdb files to BIOVIA Discovery Studio in order to calculate RMSD, as a measure of similarity among the structures. Note that there exists a significant difference (ΔRMSD>2 Angstrom) in the structures predicted by Robetta/RoseTTAFold and ColabFold/AlphaFold2. Their difference mainly stems from the coils and turns rather than the alpha helices. Without the availability of an experimentally-verified 3D structure for the enzyme, such workflow was the only logical way one could turn into to find out more about the structure of FjTAL and its relevance to its function (Table 4 and Figure 6).

Table 3: The results of secondary structure prediction and extraction.

	FjTAL_1_AF2 (Stride)	FjTAL_3_AF2 (Stride)	FjTAL_3_Rob (Stride)	FjTAL_4_AF2 (Stride)	FjTAL_4_Rob (Stride)	Sequence (JPred4)	Sequence (PROTEUS2)
# of alpha helices	19	19	18	19	18	17	18
# of 310 helices	4	5	5	5	5	N/A	N/A
# of beta strands	9	9	7	9	5	10	16

Figure 3: The secondary structures retrieved from FjTAL_1_AF2 as one of the top candidate structures. H: Alpha helix, G: 3-10 helix, I: PI-helix, E: Extended conformation (beta strand), B: Isolated bridge, T: Turn, C: Coil (none of the above).

Figure 4: Secondary structures predicted by PROTEUS2. (C: coil, E: beta strand, H: alpha helix).

Figure 5: Ribbon visualization of FjTAL_1_AF2.pdb as one of the candidate structures for FjTAL.
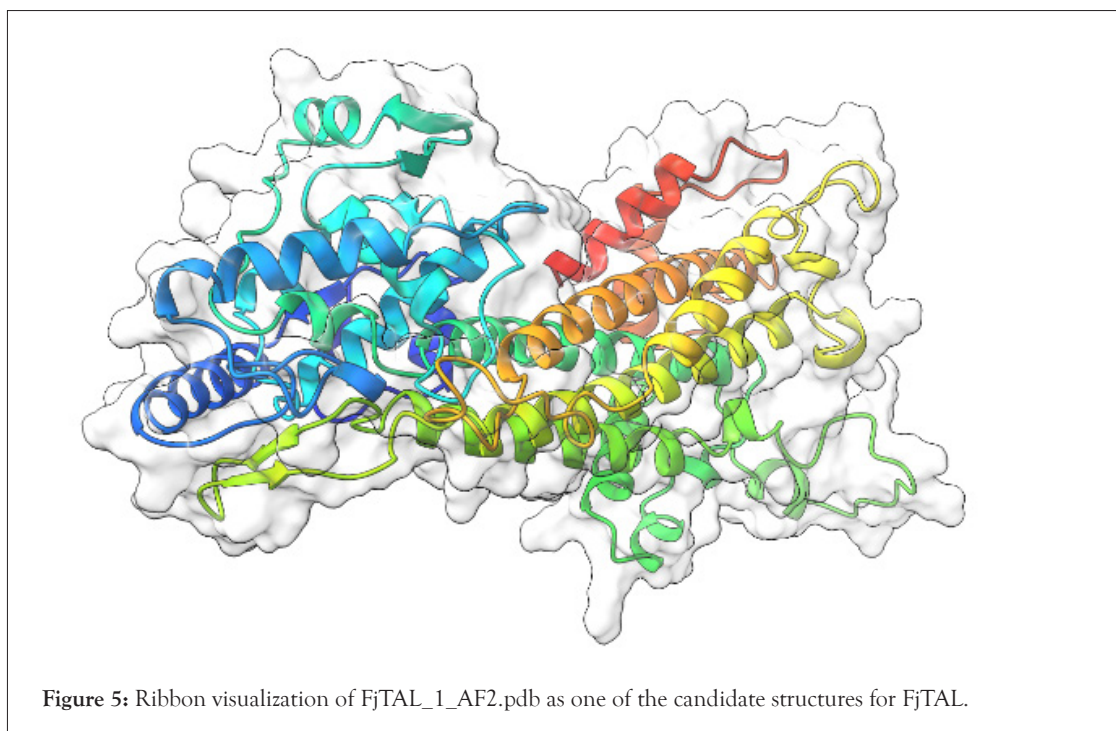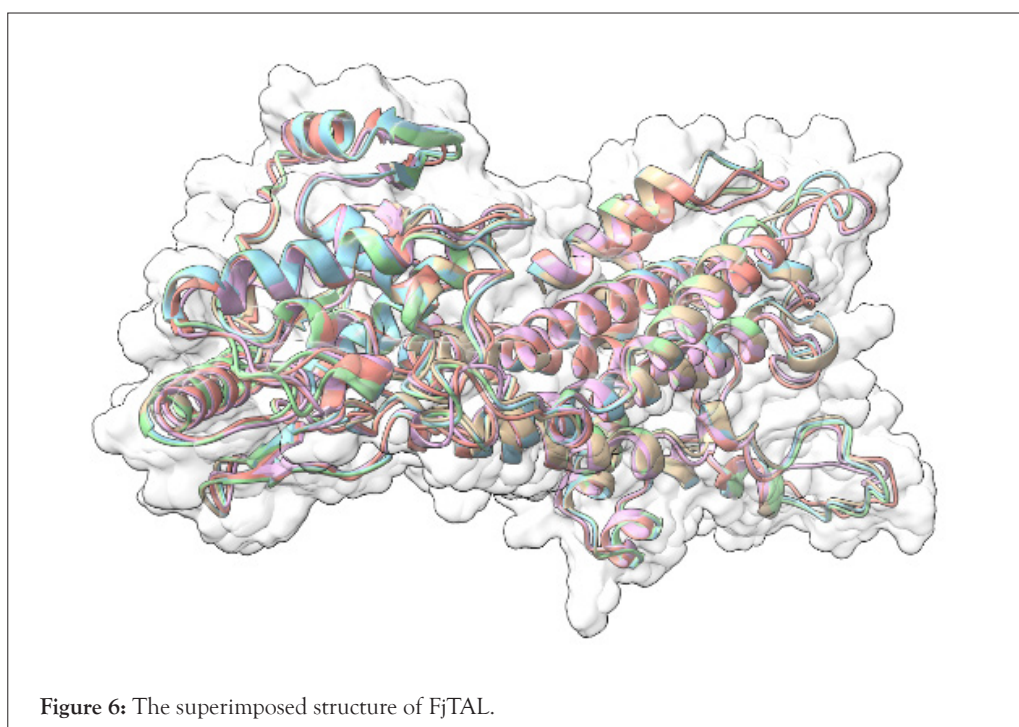
Table 4: RMSD values for each pair of models. We have arbitrarily taken FjTAL_1_AF2 as the reference model.

Molecule	C-Alpha	Main-chain	Side-chain	All protein
FjTAL_3_AF2	0.237	0.285	0.67	0.512
FjTAL_3_Rob	1.456	1.48	2.608	2.112
FjTAL_4_AF2	0.276	0.313	0.736	0.563
FjTAL_4_Rob	1.423	1.447	2.608	2.1

Figure 6: The superimposed structure of FjTAL.

FjTAL molecular docking to L-tyrosine, P-coumaric acid and caffeic acid

With the availability of the predicted structure of FjTAL, a molecular docking task was executed. The structures of ligands i.e., L-tyrosine, p-coumaric acid and caffeic acid were retrieved from ChemSpider and their structures were subsequently adjusted [27-30] to pH=7.4. Then, an MM2 minimization task was performed to retrieve the best energetically-favored representation of the ligands. The five receptor pdb files were docked with three potential ligands, L-tyrosine, p-coumaric acid and caffeic acid *via* the vina31-based docking server, CB-Dock [31-33]. CB-Dock reports five cavities and their corresponding vina score for each pair of ligand and receptor. The top results, all of which possessing a vina score=<-5.5, were selected for further investigations.

We used mol*[34] to determine the residues that constituted the binding pocket of FjTAL in each of these complexes. Interestingly two distinct binding sites, named after their first residues as VQAY and VIY cavities, consistently appeared in most of the structures (Figures 7-9).
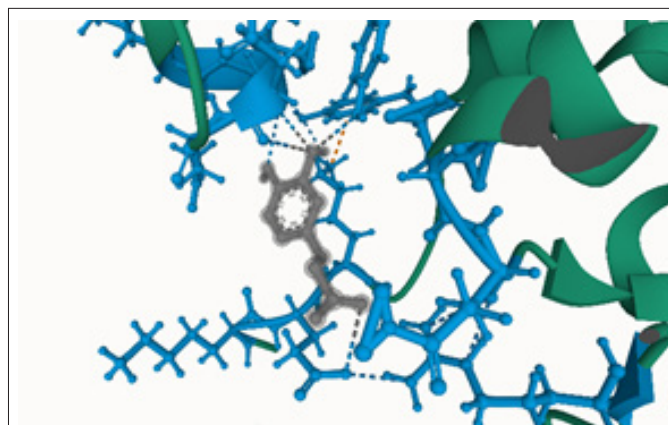

Figure 7: The predicted binding site of pH-adjusted, MM2 minimized, caffeic acid and FJTAL_1_AF2.pdb with vina score = -5.8. The blue residues depict the VQAY pocket, which is comprised of less evolutionary conserved residues.
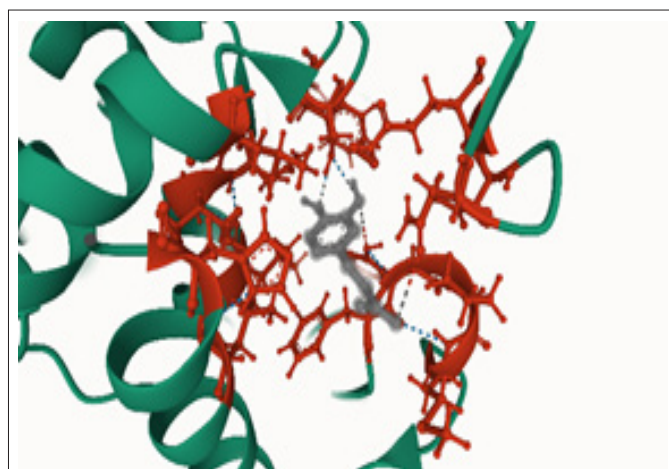

Figure 8: The predicted binding site of pH-adjusted, MM2 minimized, caffeic acid and FjTAL_1_AF2.pdb with vina score = -5.9. The red residues depict the VIY pocket, consisted of many evolutionary conserved residues.

	L-tyrosine		p-coumaric acid		caffeic acid	
FjTAL_1_AF2	-6.2	-5.7	-5.7	-5.6	-5.9	-5.8
FjTAL_3_AF2	-6	-5.7	-5.6	-5.6	-5.8	-5.8
FjTAL_3_Rob	-5.7		-6		-6.1	-5.6
FjTAL_4_AF2	-6.1	-5.7	-5.7	-5.6	-5.9	-5.6
FjTAL_4_Rob	-5.5		-5.5		-5.7	

Figure 9: The molecular docking top results and their corresponding binding cavities. VQAY cavity is in blue and VIY cavity is in red. Other colors represent rare and presumably false binding sites.

Some of the residues that constitute the VIY cavity, are known to form the prosthetic group, 3,5-dihydro-5-methylidene-4H-imidazol-4-one (MIO), which has been proved to act as an electrophilic species in the deamination reaction catalyzed by Phenylalanine Ammonia Lyase (PAL) [35]. VIY cavity homologs also appeared in the experimentally-verified structure of Rhodobacter sphaeroides Tyrosine Ammonia Lyase, RsTAL in complex with caffeate and coumarate [36]. The VQAY cavity exhibits very few evolutionary-conserved residues, suggesting that it is either completely an artifact or it could be another binding site to the ligands as well as the VIY cavity. Site directed mutagenesis studies can help us further illustrate the importance of VQAY cavity. The molecular docking results demonstrate that pHCA and caffeic acid bind to FjTAL in the same pocket as L-tyrosine, supporting the idea that these two may competitively inhibit the activity of FjTAL, and further result in a negative feedback response [6].

CONCLUSION

In this study, the 3D structure of *Flavobacterium johnsoniae* Tyrosine Ammonia Lyase (FjTAL) has been predicted by employing the state of art computational tools. The candidate structures were filtered and subsequently docked with three potential ligands, L-tyrosine, p-coumaric acid and caffeic acid. The results indicated that two potential binding cavities may exist on the surface of FjTAL, one of which exhibited great sequence identity with the experimentally-verified docking site of RsTAL. The other detected binding site may be a false positive result or a second binding site for the ligands. Eventually, site directed mutagenesis studies and X-ray crystallography data would be extremely beneficial to help us understand the structure of FjTAL comprehensively.

REFERENCES

1. Haslinger K, Prather KL. Heterologous caffeic acid biosynthesis in Escherichia coli is affected by choice of tyrosine ammonia lyase and redox partners for bacterial Cytochrome P450. Microb Cell Fact. 2020;19(1):1-2.

2. Rodrigues JL, Araújo RG, Prather KL, Kluskens LD, Rodrigues LR. Heterologous production of caffeic acid from tyrosine in Escherichia coli. Enzyme Microb Technol. 2015;71:36-44.

3. Cousins KR. ChemDraw Ultra 9.0. CambridgeSoft, 100 CambridgePark Drive, Cambridge, MA 02140. www. cambridgesoft. com. See Web site for pricing options. J Am Chem Soc. 2005;127: 4115–4116.

4. Jendresen CB, Stahlhut SG, Li M, Gaspar P, Siedler S, Förster J, et al. Highly active and specific tyrosine ammonia-lyases from diverse origins enable enhanced production of aromatic compounds in bacteria and Saccharomyces cerevisiae. Appl Environ Microbiol. 2015;81(13):4458-76.

5. Xue Z, McCluskey M, Cantera K, Ben-Bassat A, Sariaslani FS, Huang L. Improved production of p-hydroxycinnamic acid from tyrosine using a novel thermostable phenylalanine/tyrosine ammonia lyase enzyme. Enzyme Microb Technol. 2007;42(1):58-64.

6. Sariaslani FS. Development of a combined biological and chemical process for production of industrial aromatics from renewable resources. Annu Rev Microbiol. 2007;61:51-69.

7. Pagès H, Aboyoun P, Gentleman R, DebRoy S. Biostrings: Efficient Manipulation of Biological 424 Strings. Bioconductor version: Release (3.10).

8. Benkert P, Biasini M, Schwede T. Toward the estimation of the absolute quality of individual protein structure models. Bioinformatics. 2011;27(3):343-50.

9. Mariani V, Biasini M, Barbato A, Schwede T. lDDT: A local superposition-free score for comparing protein structures and models using distance difference tests. Bioinformatics. 2013;29(21):2722-8.

10. Waterhouse A, Bertoni M, Bienert S, Studer G, Tauriello G, Gumienny R, et al. SWISS-MODEL: homology modelling of protein structures and complexes. Nucleic Acids Res. 2018 ;46(W1):W296-303.

11. Bienert S, Waterhouse A, de Beer TA, Tauriello G, Studer G, Bordoli L, et al. The SWISS-MODEL Repository—new features and functionality. Nucleic Acids Res. 2017;45(D1):D313-9.

12. Kelley LA, Mezulis S, Yates CM, Wass MN, Sternberg MJ. The Phyre2 web portal for protein modeling, prediction and analysis. Nat Protoc.2015;10(6):845-58.

13. Mirdita M, Schütze K, Moriwaki Y, Heo L, Ovchinnikov S, Steinegger M. ColabFold-Making protein folding accessible to all. bioRxiv.2021.

14. Jumper J, Evans R, Pritzel A, Green T, Figurnov M, Ronneberger O, et al. Highly accurate protein structure prediction with AlphaFold. Nature. 2021;596(7873):583-9.

15. Case DA, Aktulga HM, Belfon K, Ben-Shalom I, Brozell SR, Cerutti DS, et al. Amber 2021. University of California, San Francisco; 2021.

16. Baek M, DiMaio F, Anishchenko I, Dauparas J, Ovchinnikov S, Lee GR, et al. Accurate prediction of protein structures and interactions using a three-track neural network. Science. 2021;373(6557):871-6.

17. Lüthy R, Bowie JU, Eisenberg D. Assessment of protein models with three-dimensional profiles. Nature. 1992;356(6364):83-5.

18. Bowie JU, Lüthy R, Eisenberg D. A method to identify protein sequences that fold into a known three-dimensional structure. Science. 1991;253(5016):164-70.

19. Colovos C, Yeates TO. Verification of protein structures: Patterns of nonbonded atomic interactions. Protein Sci. 1993;2(9):1511-9.

20. Haas J, Gumienny R, Barbato A, Ackermann F, Tauriello G, Bertoni M, et al. Introducing "best single template" models as reference baseline for the Continuous Automated Model Evaluation (CAMEO). Proteins Struct Funct Bioinforma. 2019 ;87(12):1378-87.

21. Robin X, Haas J, Gumienny R, Smolinski A, Tauriello G, Schwede T. Continuous Automated Model EvaluatiOn (CAMEO)—Perspectives on the future of fully automated evaluation of structure prediction methods. Proteins Struct Funct Bioinforma.2021;89(12):1977-86.

22. Frishman D, Argos P. Knowledge-based protein secondary structure assignment. Proteins Struct. Funct. Bioinforma. 1995;23(4):566-79.

23. Drozdetskiy A, Cole C, Procter J, Barton GJ. JPred4: A protein secondary structure prediction server. Nucleic Acids Res. 2015;43(W1):W389-94.

24. Montgomerie S, Cruz JA, Shrivastava S, Arndt D, Berjanskii M, Wishart DS. PROTEUS2: A web server for comprehensive protein structure prediction and structure-based annotation. Nucleic Acids Res. 2008;36(suppl_2):W202-9.

25. Pettersen EF, Goddard TD, Huang CC, Meng EC, Couch GS, Croll TI, et al. UCSF ChimeraX: Structure visualization for researchers, educators, and developers. Protein Sci. 2021;30(1):70-82.

26. Goddard TD, Huang CC, Meng EC, Pettersen EF, Couch GS, Morris JH, et al. UCSF ChimeraX: Meeting modern challenges in visualization and analysis. Protein Sci. 2018;27(1):14-25.

27. O'Boyle NM, Banck M, James CA, Morley C, Vandermeersch T, Hutchison GR. Open Babel: An open chemical toolbox. J Cheminform. 2011;3(1):1-4.

28. O'Boyle NM, Morley C, Hutchison GR. Pybel: A Python wrapper for the OpenBabel cheminformatics toolkit. Chem Cent J. 2008;2(1):1-7.

29. Bray SA, Lucas X, Kumar A, Grüning BA. The ChemicalToolbox: Reproducible, user-friendly cheminformatics analysis on the Galaxy platform. J Cheminform. 2020;12(1):1-7.

30. Afgan E, Baker D, Batut B, Van Den Beek M, Bouvier D, Čech M, et al. The Galaxy platform for accessible, reproducible and collaborative biomedical analyses: 2018 update. Nucleic Acids Res. 2018;46(W1):W537-44.

31. Trott O, Olson AJ. AutoDock Vina: Improving the speed and accuracy of docking with a new scoring function, efficient optimization, and multithreading. J Comput Chem. 2010;31(2):455-61.

32. Liu Y, Grimm M, Dai WT, Hou MC, Xiao ZX, Cao Y. CB-Dock: A web server for cavity detection-guided protein–ligand blind docking. Acta Pharmacol Sin. 2020;41(1):138-44.

33. Cao Y, Li L. Improved protein–ligand binding affinity prediction by using a curvature-dependent surface-area model. Bioinformatics. 2014;30(12):1674-80.

34. Sehnal D, Bittrich S, Deshpande M, Svobodová R, Berka K, Bazgier V, et al. Mol* Viewer: Modern web app for 3D visualization and analysis of large biomolecular structures. Nucleic Acids Res. 2021;49(W1):W431-7.

35. Calabrese JC, Jordan DB, Boodhoo A, Sariaslani S, Vannelli T. Crystal structure of phenylalanine ammonia lyase: multiple helix dipoles implicated in catalysis. Biochemistry. 2004;43(36):11403-16.

36. Louie GV, Bowman ME, Moffitt MC, Baiga TJ, Moore BS, Noel JP. Structural determinants and modulation of substrate specificity in phenylalanine-tyrosine ammonia-lyases. Chem Biol. 2006 ;13(12):1327-38.